IAI Journals.ASM.org

The Phosphoenolpyruvate Phosphotransferase System in Group A *Streptococcus* Acts To Reduce Streptolysin S Activity and Lesion Severity during Soft Tissue Infection

Kanika Gera,[a] Tuquynh Le,[a] Rebecca Jamin,[b] Zehava Eichenbaum,[b] Kevin S. McIver[a]

Department of Cell Biology & Molecular Genetics and Maryland Pathogen Research Institute, University of Maryland, College Park, Maryland, USA[a]; Biology Department, Georgia State University, Atlanta, Georgia, USA[b]

Obtaining essential nutrients, such as carbohydrates, is an important process for bacterial pathogens to successfully colonize host tissues. The phosphoenolpyruvate phosphotransferase system (PTS) is the primary mechanism by which bacteria transport sugars and sense the carbon state of the cell. The group A streptococcus (GAS) is a fastidious microorganism that has adapted to a variety of niches in the human body to elicit a wide array of diseases. A Δ*ptsI* mutant (enzyme I [EI] deficient) generated in three different strains of M1T1 GAS was unable to grow on multiple carbon sources (PTS and non-PTS). Complementation with *ptsI* expressed under its native promoter in single copy was able to rescue the growth defect of the mutant. In a mouse model of GAS soft tissue infection, all Δ*ptsI* mutants exhibited a significantly larger and more severe ulcerative lesion than mice infected with the wild type. Increased transcript levels of *sagA* and streptolysin S (SLS) activity during exponential-phase growth was observed. We hypothesized that early onset of SLS activity would correlate with the severity of the lesions induced by the Δ*ptsI* mutant. In fact, infection of mice with a Δ*ptsI sagB* double mutant resulted in a lesion comparable to that of either the wild type or a *sagB* mutant alone. Therefore, a functional PTS is not required for subcutaneous skin infection in mice; however, it does play a role in coordinating virulence factor expression and disease progression.

The ability to obtain essential nutrients during an infection is critical for bacterial pathogens to successfully colonize and proliferate within host tissues. One such key process involves the ability to import and catabolize optimal carbon sources such as carbohydrates. Bacteria have evolved elegant regulatory pathways that detect the presence of preferred carbohydrates, repress the utilization of nonpreferred sugars, and regulate their metabolism based on this information flow (1, 2). In fact, many pathogens tightly control the genes involved in carbohydrate utilization and regulation in response to *in vivo* growth, and these same genes have been shown to be important to the disease process (3–8). Therefore, it is apparent that bacterial pathogens have closely linked their sugar metabolic sensing networks to virulence gene expression during infection.

The primary bacterial system coupling the transport of carbohydrates across the cytoplasmic membrane with their phosphorylation is a multiprotein phosphorelay called the phosphoenolpyruvate (PEP)-dependent phosphotransferase system (PTS) (9). The PTS is composed of at least three distinct proteins: the cytosolic proteins enzyme I (EI) and Hpr, encoded by *ptsI* and *ptsH*, respectively, and the membrane-bound sugar-specific enzyme II (EII) proteins. Each EII consists of one or two integral membrane-bound domains (EIIC/EIID) that are necessary for sugar translocation, and these domains form complexes with two hydrophilic components (EIIA and EIIB) that are required for substrate phosphorylation (1, 10). EI initiates the phosphorelay after autophosphorylation by PEP, followed by transfer of the phosphoryl group to the histidine at position 15 of HPr. P∼HPr–His then donates the phosphoryl group to one of several sugar-specific EIIA proteins, which in turn transfers it to its cognate EIIB, and finally onto the incoming cognate sugar transported by EIIC/D.

In addition to carbohydrate transport, the PTS in Gram-positive bacteria also plays an important role in modulating the activity of transcriptional regulators (e.g., antiterminators, activators) that control expression of sugar utilization genes. The PTS intermediates P∼HPr–His and P∼EII^{sugar} can directly phosphorylate transcriptional regulators that contain either PTS regulatory domains (PRD) and/or EII-like domains to affect their activity. In *Bacillus subtilis*, the phosphorylation state of EI and Hpr regulates the activity of PRD-containing antiterminators (e.g., LicT) and activators (e.g., LevR) in response to glucose availability, thus controlling their ability to regulate the expression of alternative sugar operons (1, 11). PTS-mediated signaling can also influence virulence gene expression in Gram-positive pathogens. The cellobiose PTS of *Streptococcus pneumoniae* is important for virulence in a murine pneumonia/sepsis model (12). Inactivation of *ptsI* (EI) and *ptsH* (Hpr) in *Clostridium difficile* led to induction of toxin gene expression in the presence of glucose (13). Activity of PrfA, the major virulence regulator in *Listeria monocytogenes*, is controlled by the phosphorylation state of PTS components (14). The *Bacillus anthracis* AtxA master virulence regulator contains both PRD and EIIB domains and requires an intact PTS pathway for full activity (15).

The PTS is also involved in carbon catabolite repression (CCR)

Received 7 October 2013 **Returned for modification** 3 November 2013
Accepted 19 December 2013
Published ahead of print 30 December 2013
Editor: A. Camilli
Address correspondence to Kevin S. McIver, kmciver@umd.edu.
Supplemental material for this article may be found at http://dx.doi.org/10.1128/IAI.01271-13.
Copyright © 2014, American Society for Microbiology. All Rights Reserved.
doi:10.1128/IAI.01271-13

via Hpr kinase (HprK)-mediated phosphorylation at Ser46 of Hpr in Gram-positive bacteria. In the presence of glucose, P~Hpr-Ser interacts with the catabolite control protein CcpA, which is then able to bind to *cre* sites found in promoters of sugar utilization and metabolism operons to mediate CCR (1, 16). In addition to its central role in CCR, CcpA has been shown be important for the virulence of a number of important Gram-positive pathogens (17–22). CcpA-independent pathways for CCR also exist in *Streptococcus mutans*, which is exerted through a network of PTS permeases (23). Thus, the sugar status of the bacterial cell can have a profound impact on virulence and expression of important virulence phenotypes in Gram-positive pathogens.

The group A streptococcus (GAS) (*Streptococcus pyogenes*) is a Gram-positive human-adapted pathogen with the ability to cause benign and life-threatening diseases in various host niches, including the respiratory tract (pharyngitis), skin (impetigo), deep tissues (necrotizing fasciitis), and bloodstream (streptococcal toxic shock syndrome). A conservative estimate indicates that more than 745 million cases of GAS infection occur worldwide each year, leading to over half a million deaths (24). The clinical impact of GAS is based largely on its ability to produce a large array of surface-exposed (e.g., M protein, capsule) and secreted (e.g., streptolysins [SLS {streptolysin S} and SLO], SpeB protease) virulence factors that contribute significantly to its pathogenesis. GAS exhibits coordinate regulation of its virulence genes in response to changing host environments through global regulatory networks such as the stand-alone regulator Mga and the two-component system (TCS) CovRS. Mutations in the histidine kinase CovS are associated with an invasive GAS disease phenotype and the altered regulation of virulence genes, including *sagA* (SLS), *speB* (cysteine protease), and *hasA* (capsule).

GAS is a fermentative lactic acid bacterium that relies heavily on sugar metabolism for its energy production, since it lacks the necessary enzymes for a functional tricarboxylic acid (TCA) cycle and oxidative cytochromes for electron transport. Early studies established that glucose, sucrose, maltose, galactose, and mannose could support growth of an M3 GAS strain (25). The addition of PTS-transported sugars such as glucose, sucrose, or trehalose to a semisynthetic growth medium stimulates the synthesis of M protein, an important GAS virulence factor involved in resistance to phagocytosis and adherence to host tissues (26). Furthermore, genes involved in carbohydrate uptake and utilization are upregulated *in vivo* and contribute to virulence in GAS models of infection (19, 21, 27, 28). CcpA-mediated CCR via Hpr is also important for GAS virulence, regulating over 6% of the genome, including indirectly repressing transcription of the *sag* operon encoding SLS (18, 19, 21). Finally, we have recently shown that the Mga virulence regulator contains PRD domains that are phosphorylated by the PTS to control Mga-regulated gene expression and virulence (3). Despite the increasing evidence that carbohydrate utilization influences GAS pathogenesis, the roles of PTS transport and signaling on disease progression have not been investigated.

In this study, we characterize the PTS pathway in multiple strains of GAS by creating a deletion mutant of *ptsI* (EI), the first protein of the phosphorelay. We show that a functional PTS is not necessary for eliciting a GAS subcutaneous soft tissue infection. However, it does limit lesion severity at the site of subcutaneous (s.c.) infection in mice by regulating the temporal expression level of streptolysin S. Thus, PTS transport and signaling contributes to GAS pathogenesis.

TABLE 1 Bacterial strains and plasmids used in this study

Bacterial strain or plasmid	Relevant genotype or description	Reference or source
E. coli strains		
DH5	*hsdR17 recA1 gyrA endA1 relA1*	56
C41(DE3)	F$^-$ *ompT gal dcm hsdS*$_B$(r_B^- m_B^-) (DE3)	57
S. pyogenes strains		
MGAS5005	M1T1 *covS*	29
5448	M1T1	58
5448AP	M1T1 *covS*	58
MGAS5005.Δ*ptsI*	Δ*ptsI* mutant in strain MGAS5005	This study
MGAS5005.Δ*ptsIc*	Δ*ptsI* complemented with pKSM456 insertion	This study
5448.Δ*ptsI*	Δ*ptsI* mutant in strain 5448	This study
5448AP.Δ*ptsI*	Δ*ptsI* mutant in strain 5448AP	This study
Plasmids		
pCRK	Temperature-sensitive conditional vector; Km^r	59
pBluescript II KS(−)	ColE1 ori Amp^r *lacZa*	Stratagene
pSL60-1	Vector containing nonpolar *aad9* gene	33
pKSM645	Δ*ptsI* mutagenic plasmid; nonpolar *aad9*	3
pBlue.Δ*ptsI*	Δ*ptsI* in pBluescript II KS(−); *bla* (Ap^r)	3
pKSM456	Promoterless *ptsI* integration plasmid; Km^r	This study

MATERIALS AND METHODS

Bacterial strains and media. *Streptococcus pyogenes* MGAS5005 (*covS*) is an invasive M1T1 strain with an available genome sequence (29). GAS strain 5448 is also an M1T1 strain isolated from an invasive infection, and 5448AP is an isogenic animal-passaged *covS* variant. GAS bacteria were either cultured in complete Todd-Hewitt medium (Alpha Biosciences) supplemented with 0.2% yeast extract (THY) or in 2× chemically defined medium (CDM) prepared by MP Biomedical as previously described (30, 31). Prior to use, freshly prepared sodium bicarbonate (59.51 μM [final concentration]) and L-cysteine (11.68 μM [final concentration]) were added along with a carbohydrate source at a final concentration of either 0.5% (D-glucose) or 1% (all other sources). Growth of GAS was assayed by measuring absorbance using a Klett-Summerson colorimeter (A filter). Alternatively, overnight cultures of GAS (10 ml) were adjusted to an optical density at 600 nm (OD_{600}) of 0.2 in saline, the appropriate carbohydrate was added, and 50-μl aliquots were transferred to the wells on a 24-well microplate (Corning) containing CDM with various sugars and covered with sealing tape (Bio-Rad). Growth was monitored for 12 to 24 h at 37°C using a FLUOstar Omega microplate spectrophotometer (BMG), with measurements taken at 30-min intervals after shaking (10 s). *Escherichia coli* strain DH5α and C41(DE3) were used as the host for plasmid constructions (Table 1). All *E. coli* strains were grown in Luria-Bertani (LB) broth (EMD Chemicals).

Antibiotics were used at the following concentrations: erythromycin at 500 μg/ml for *E. coli* and 1.0 μg/ml for GAS, spectinomycin at 100 μg/ml for both *E. coli* and GAS, and kanamycin at 50 μg/ml for *E. coli* and 300 μg/ml for GAS.

DNA manipulations. Plasmid DNA was isolated from *E. coli* using the Wizard Plus SV miniprep system (Promega). DNA fragments were gel purified from agarose using the QIAquick gel extraction kit (Qiagen) or

TABLE 2 Primers used in this study

Target gene	PCR primer	Sequence (5′–3′)[a]	Reference
ptsI	ptsI-1a	agatctGCTGAGTGACTTGTACGA	This study
	ptsI-1b	GGTATTCATGCGCGTCCA	This study
	ptsI-2a	gcgGCCTTGTGTTGGTGGTTTAAGAGCAAC	This study
	ptsI-2b	*GTCACTCAGC*agatctCGTGCGCTTACAGAATGT	This study
	ptsI-3a	tctagaGCGGCCTTGTGTTGGTGGTTT	This study
	ptsI-3b	ctcgagGGTATTCATGCGCGTCCA	This study
	ptsl-internal sense	CAAATTGGTCTGCAAGC	This study
	ptsl-internal antisense	CAGATACTGCTCAACTTAACA	This study
	ptsl-external sense	GCTAGCAAAAAAGAGCTGGTTTA	This study
	ptsl-external antisense	CTCTTGACTACAAAGGTAAAGCAGTAAA	This study
	5005.645jxn-sense	GCGGGTTATTTTTTAAATGTTTCCGAAG	This study
	5005.645jxn-antisense	GGGCCATCTGCAAAATACAAAGCAT	This study
	ptsIcomplementL	cccggatccCATCACTCTTGACTACAA	This study
	ptsIcomplementR	cccggatccTTAATCTTCAGAAACGTA	
	ptsI M1 RT L	CGGAAACCAAGGAATGGAT	This study
	ptsI M1 RT R	TGGCAAACCTGTTGTGGTT	
aad9	aad9L2-bglII	gcgcagatctGGGTGACTAAATAGTGAGGAG	19
	aad9R2-bglII	gcgcagatctGGCATGTGATTTTCC	
gyrA	gyrA M1 RT L	CGACTTGTCTGAACGCCAAAGT	60
	gyrA M1 RT R	ATCACGTTCCAAACCAGTCAAAC	
sagA	sagA M1 RT L	GCTACTAGTGTAGCTGAAACAACTCAA	19
	sagA M1 RT R	AGCAACAAGTAGTACAGCAGCAA	

[a] Lowercase letters indicate nucleotides not complementary to the target DNA; underlining indicates restriction sites. Italic nucleotides are in the overlap region for SOEing.

the Wizard SV gel and PCR clean-up system (Promega). PCR for cloning and generating probes was performed using Phusion (Finnzymes) according to the manufacturer's protocol. All DNA sequencing was done by Genewiz, Inc. Genomic DNA was extracted from GAS using the MasterPure complete DNA and RNA purification kit for Gram-positive bacteria (Epicentre).

Construction of a Δ*ptsI* mutant in GAS. The plasmid to generate the Δ*ptsI* allele was created as previously described (3). Briefly, the primers ptsI-1a and ptsI-1b (Table 2) were used to amplify from *S. pyogenes* MGAS5005 genomic DNA (gDNA) an 819-bp upstream region containing 578 bp of *ptsI* and a BglII restriction site. Primers ptsI-2a and ptsI-2b (Table 2) were used to amplify an 812-bp region containing the 3′ end of *ptsI* with BglII ends and a 10-bp overlap with the first fragment at the 5′ end. These fragments were combined as the template DNA for PCR splicing by overlap extension (SOEing) (32) with primers ptsI-3a and ptsI-3b (Table 2) to generate the *ptsI* deletion. The resulting product was blunt end ligated into pBluescript II KS(−) to create pBlueΔ*ptsI* (Table 1). The nonpolar *aad9* spectinomycin resistance cassette was amplified from pSL60-1 using primers aad9L2-bglII and aad9R2-bglII (Table 2), digested with BglII, and ligated into BglII-digested pBlueΔ*ptsI* (Table 1). The resulting XbaI/XhoI Δ*ptsI*::*aad9* fragment from pBlueΔ*ptsI* was ligated into XbaI/XhoI-digested pCRK to yield pKSM645, which was used to construct the Δ*ptsI* mutant MGAS5005.Δ*ptsI* (Table 1). Additional mutants were constructed from strain 5448 (5448.Δ*ptsI* and 5448AP [5448AP.Δ*ptsI*]) using the same protocol (Table 1). GAS Δ*ptsI* mutants were screened for sensitivity to kanamycin and verified by PCR on genomic DNA for specific junction regions.

Single-copy complementation of strain MGAS5005.Δ*ptsI*. A thermosensitive integration plasmid for single-copy complementation was constructed using primers ptsIcomplementL and ptsIcomplementR (Table 2) to amplify a 1,919-bp fragment containing a promoterless wild-type copy of *ptsI* and BamHI restriction site on both ends. The resulting PCR fragment was digested with BamHI, ligated into BamHI-digested pCRK to yield pKSM456 (Table 1), and confirmed by sequence analysis. pKSM456 was electroporated into the mutant MGAS5005.Δ*ptsI* at the permissive temperature (30°C), and integrants were isolated following growth at the nonpermissive temperature (37°C) to allow for complementation of the Δ*ptsI* allele in single copy. The resulting strain MGAS5005.Δ*ptsIc* was verified by PCR and sequence analysis.

Murine infections. An overnight culture (10 ml) was used to inoculate 75 ml of THY and incubated statically at 37°C until late logarithmic phase. Approximately 3×10^9 CFU/ml, as determined by microscope counts and verified by plating for viable colonies, were used to infect 5- to 6-week-old female CD1 mice (Charles River Laboratories). The mice were anesthetized with ketamine, hair was removed from an ~3-cm^2 area of the haunch with Nair (Carter Products), and 100 μl of a cell suspension in saline (3×10^8 CFU/mouse) was injected subcutaneously (s.c.). Mice were monitored twice daily for 7 days and were euthanized by CO_2 asphyxiation upon signs of morbidity. Lesion sizes ($L \times W$) were measured at 36 h postinfection with length (L) determined at the longest point of the lesion and width (W) as the widest point. Lesion size data were analyzed using GraphPad Prism (GraphPad Software) and tested for significance using an unpaired two-tailed t test with 99% confidence.

RNA isolation. GAS from an overnight culture was inoculated 1:20 into 10 ml THY supplemented with appropriate antibiotics and grown to the appropriate Klett unit (ca. 80 to 100). The cells were then pelleted by centrifugation at 8,000 × *g* for 20 min at 4°C. The cells were resuspended in 1 ml of TE buffer (10 mM Tris [pH 7.4] and 1 mM EDTA) with 0.2% (vol/vol) Triton X-100 and boiled for 10 min. The lysate was extracted three times using chloroform-isoamyl alcohol, ethanol (EtOH) precipitated for 20 min at −80°C, and pelleted at 13,000 × *g* for 15 min at 4°C, and the RNA pellet was resuspended in diethyl pyrocarbonate (DEPC)-treated H_2O. RNA quality was assessed on a formaldehyde gel. The formaldehyde gel consisted of 18% (vol/vol) formaldehyde, 1% (wt/vol) agarose, 72% (vol/vol) DEPC-treated H_2O, and 10% (vol/vol) 10× MOPS buffer [10× MOPS buffer is 0.4 M 3-(*N*-morpholino)propanesulfonic acid (MOPS) (pH 7.0), 0.1 M sodium acetate, 0.01 M EDTA]). To quantify RNA, absorbance at 260/280 nm was determined using a spectrophotometer. RNA (5 μg) was treated with DNase using the Turbo DNA Free kit (Ambion) per the manufacturer's protocol. Treated RNA was assessed

for quality as mentioned above and for gDNA contamination by PCR analysis.

Real-time RT-PCR. Twenty-five nanograms of DNase-treated total RNA was added to SYBR green master mix (Applied Biosystems) along with 6.5 μl of each gene-specific real-time primer from a stock of 20 nM (Table 2) using the one-step protocol. The real-time reverse transcription-PCR (RT-PCR) experiments were completed using a Light Cycler 480 (Roche), and the levels presented represent ratios of the wild type/experimental levels relative to the level of *gyrA* transcript as the internal control. The real-time primers were designed using Primer3, the WWW primer tool (biotools.umassmed.edu/bioapps/primer3_www.cgi).

Biolog phenotype microarrays. Carbohydrate metabolic profiles were determined using the Biolog Omnilog system (Biolog Inc.) per the manufacturer's protocol. Tests were performed utilizing the PM1 and PM2 carbon panels, each as standard 96-well microplates containing 95 different carbon sources and one negative control. Each well contained a redox dye for colorimetric determination in response to metabolizing the carbon source. Strains were first cultured on tryptic soy agar (TSA) 5% blood agar plates for 24 h at 37°C. The cells were swabbed, picked off the plate, and resuspended in inoculating fluid (Biolog) to adjust to an absorbance at 600 nm of 0.14. An aliquot of 100 μl of the suspension was immediately dispensed into each well of the PM microplate with a multichannel pipette. The plate was incubated at 37°C for 48 h, and the data were analyzed using the Omnilog software (Biolog).

Hemolysis assay. GAS bacteria were grown in THY supplemented with 10% heat-inactivated horse serum (Sigma). Samples were taken every hour for a total of 8 to 14 h and immediately frozen at −80°C, bacterial cells were pelleted, and a 1:10 dilution was made of the supernatant in saline. Five hundred microliters of the diluted supernatant was added to an equal volume of 2.5% (vol/vol) difibrinated sheep red blood cells (RBC) (Sigma) and washed three times with sterile phosphate-buffered saline (PBS), pH 7.5. This mixture was incubated at 37°C for 1 h and cleared by centrifugation at 3,000 × *g*. Supernatants were measured at 541 nm by using a spectrophotometer (Molecular Dynamics) to determine release of hemoglobin by lysed RBCs. Percent hemolysis was defined as follows: [(sample *A* − blank *A*)/(100% lysis *A*)] × 100, where *A* is absorbance. To assay for streptolysin O-specific hemolytic activity, the streptolysin S inhibitor trypan blue (13 μg/μl) was added to samples prior to incubation.

RESULTS

GAS EI mutant (Δ*ptsI*) is defective for growth in several carbohydrates. To assess the role of the PEP phosphotransferase system (PTS) in GAS, an EI mutant (Δ*ptsI*) was constructed in the M1T1 strain MGAS5005 (Table 1), a representative strain of the most common GAS serotype associated with severe invasive disease worldwide (29). The genetic composition of the PTS in GAS is comparable to that found in many bacterial species (1). The "general" PTS proteins Hpr (encoded by *ptsH*) and EI (encoded by *ptsI*) are highly conserved among low-G+C Gram-positive bacteria, including multiple species of *Streptococcus*. The *ptsHI* (M5005_Spy1121 and M5005_Spy1120, respectively) genes are typically found in an operon (Fig. 1A). We replaced wild-type *ptsI* with an in-frame deletion (Δ*ptsI*) containing a nonpolar *aad9* spectinomycin resistance cassette (33) in the MGAS5005 genome (Fig. 1A). The resulting MGAS5005.Δ*ptsI* mutant (Table 1) was verified by PCR (data not shown) and qRT-PCR (see Fig. 4A). The MGAS5005.Δ*ptsI* strain exhibited a small-colony phenotype compared to wild-type MGAS5005 when grown on TSA agar supplemented with 5% sheep blood, but not on TSA or THY agar alone (data not shown). Although the MGAS5005.Δ*ptsI* strain had a slightly increased lag phase compared to the lag phase of the wild type in rich THY medium, the growth kinetics were comparable (data not shown).

Growth of the parental MGAS5005 strain and the MGAS5005.Δ*ptsI* mutant was further analyzed by phenotypic microarray (Biolog) using the PM1 and PM2 carbon panels, which contain a total of 190 different carbon sources. Each well was inoculated with either strain, and the plates were incubated at 37°C in an Omnilog plate incubator for 48 h to allow generation of independent metabolic curves (data not shown). Wild-type MGAS5005 showed reasonable metabolism on multiple carbon sources (Table 3). Of the 45 carbon sources able to support MGAS5005 metabolism, the Δ*ptsI* mutant showed poor or no utilization of 19 carbon sources (Table 3), including both PTS-transported (boldface) and non-PTS-transported sugars. Carbohydrate-specific phenotypes observed by phenotype microarray were confirmed by growth assays in chemically defined medium (CDM) supplemented with 1% (wt/vol) of certain carbohydrate sources as the sole carbon source. MGAS5005.Δ*ptsI* showed comparable growth to MGAS5005 (wild type) when grown in CDM supplemented with 0.5% glucose (Fig. 1B). However, MGAS5005.Δ*ptsI* was unable to grow when the PTS-transported sugars sucrose and fructose (Fig. 1C and D and Table 3) or lactose, galactose, trehalose, and mannose were tested using CDM (Table 3 and data not shown). These results strongly support the idea that MGAS5005.Δ*ptsI* lacks a functional PTS. The inability of the Δ*ptsI* mutant to grow on some non-PTS sugars (Table 3) indicates the importance of a functional PTS for uptake and utilization of non-PTS sugars.

To confirm that the growth defect phenotype was specific to the Δ*ptsI* allele, we generated a complemented Δ*ptsI* strain by introducing a wild-type *ptsI* allele into the chromosome of the MGAS5005.Δ*ptsI* strain (MGAS5005.Δ*ptsI*c [Table 1]). The MGAS5005.Δ*ptsI*c complemented strain showed a growth profile in all PTS-specific sugars comparable to wild-type MGAS5005 (Fig. 1C and D and data not shown).

The Δ*ptsI* mutant shows increased soft tissue damage in a mouse model of GAS skin infection. The roles of EI (*ptsI*) and PTS in GAS virulence was assessed using a murine model of streptococcal soft tissue infection. The MGAS5005 and MGAS5005.Δ*ptsI* strains were grown to late log phase and then injected subcutaneously (~3×10^8 CFU) into the haunches of 5- to 6-week-old, female CD1 mice. For 7 days postinfection, the progression of disease was monitored for both lesion size (at 38 h postinfection) and survival. Mice infected with wild-type MGAS5005 developed purulent abscessed lesions with minimal ulceration after 38 h (Fig. 2A). In contrast, mice infected with a comparable dose of MGAS5005.Δ*ptsI* developed lesions at 16 h equivalent in size to the lesions of mice infected with the wild type at 38 h, and these lesions became fully ulcerative by 24 h postinfection (data not shown). The visual differences in both the size and severity of lesions between the wild type and the Δ*ptsI* mutant at 38 h postinfection were quite striking (Fig. 2A). This coincided with a significant increase in the mean lesion size for mice infected with MGAS5005.Δ*ptsI* compared to MGAS5005 measured at the same time postinfection (Fig. 2B). Interestingly, a corresponding increase in lethality over 7 days was not observed in mice infected with MGAS5005.Δ*ptsI*, suggesting that there was no enhancement of dissemination from the skin or in systemic lethality (Fig. 2C). Thus, the Δ*ptsI* mutant exhibits a hypervirulent phenotype at the site of infection compared to the wild type; however, systemic progression and lethality are not altered.

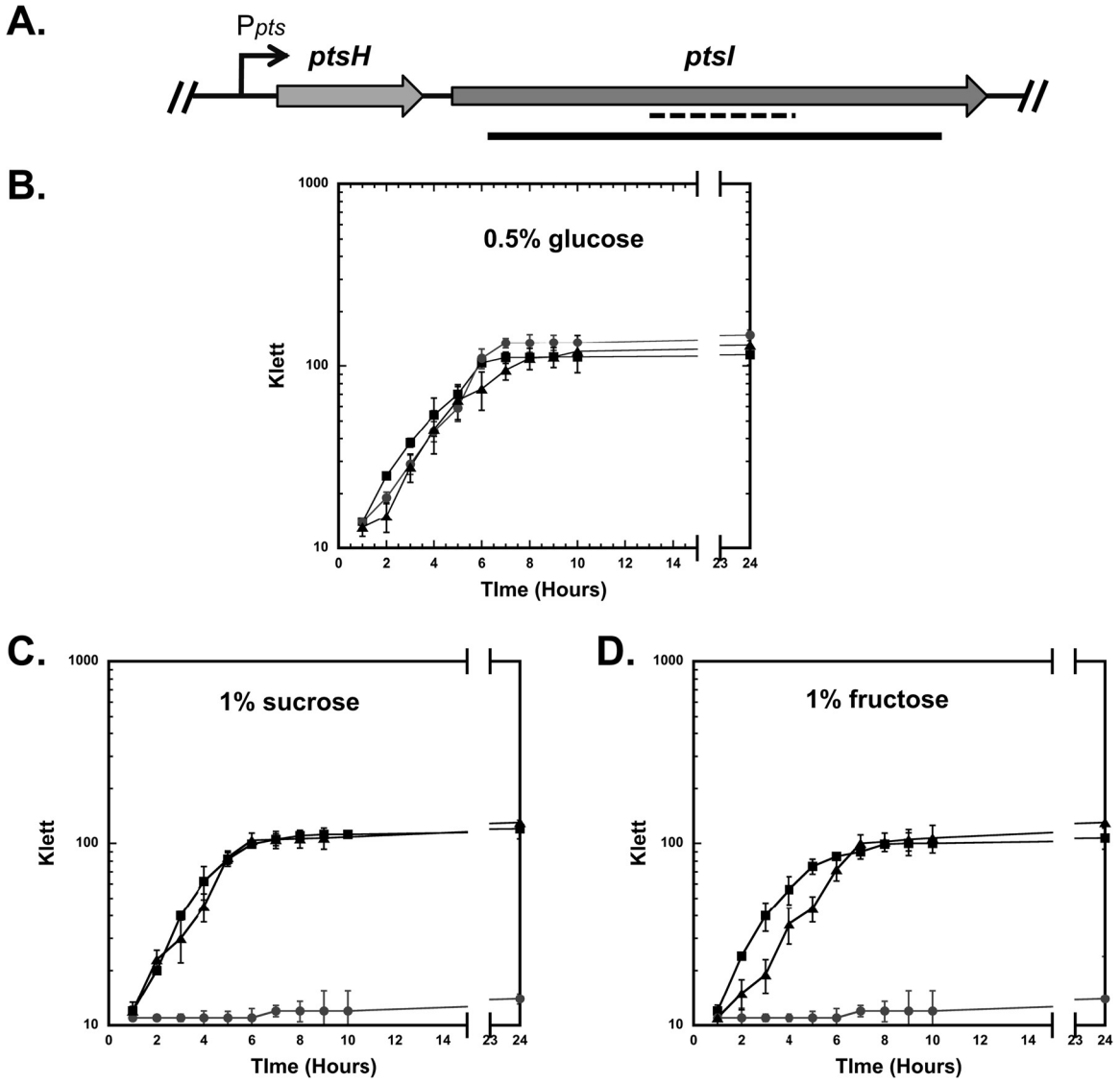

FIG 1 Construction of a Δ*ptsI* mutant from the MGAS5005 strain. (A) Schematic of the *ptsHI* genomic region from GAS MGAS5005 with the putative P*pts* promoter (arrow) driving transcription of *ptsH* (Hpr) and *ptsI* (EI). The Δ*ptsI* region (black bar) was replaced with a nonpolar *aad9* cassette (spectinomycin resistance). The region amplified for qRT-PCR analysis is shown (dashed line). (B to D) Growth curves of wild-type MGAS5005 (black squares), Δ*ptsI* mutant (gray circles), and complemented Δ*ptsI* (black triangles) in CDM supplemented with 0.5% (wt/vol) glucose (B), 1% (wt/vol) sucrose (C), or 1% (wt/vol) fructose (D) are shown. Bacterial growth is measured by absorbance in Klett units on the *y* axes. Data are representative of three independent experiments.

The Δ*ptsI* mutant exhibits a comparable phenotype in multiple M1T1 GAS strains. To explore the role of EI in different genetic backgrounds, we constructed independent Δ*ptsI* mutants in two additional M1T1 strains, strains 5448 and 5448AP (*covS*), with the same mutagenic plasmid used for MGAS5005.Δ*ptsI* (Table 1). Similar to MGAS5005.Δ*ptsI*, a small-colony phenotype on blood agar plates was observed for 5448.Δ*ptsI* and 5448AP.Δ*ptsI* (data not shown). Furthermore, these Δ*ptsI* mutants exhibited growth defects when grown in CDM supplemented with PTS sugars identical to that seen for MGAS5005.Δ*ptsI* (see Fig. S1 in the supplemental material; also data not shown). Finally, similar growth phenotypes were observed in at least two independently isolated MGAS5005.Δ*ptsI* strains, the 5448.Δ*ptsI* and 5448AP.Δ*ptsI* mutant strains. Thus, biologically independent Δ*ptsI* mutants exhibit comparable phenotypes in multiple M1T1 backgrounds.

We also tested the 5448.Δ*ptsI* and 5448AP.Δ*ptsI* mutants and their respective parental strains in the murine model of streptococcal soft tissue infection (Fig. 3). As seen with MGAS5005.Δ*ptsI*, mice infected by either Δ*ptsI* mutant exhibited a more severe (Fig. 3A) and significantly larger (Fig. 3B) ulcerative lesion at 38 h postinfection compared to infection with its parental strain. In contrast to MGAS5005.Δ*ptsI* and 5448AP.Δ*ptsI* (*covS* mutants), only mice infected with 5448.Δ*ptsI* (intact *covS*) showed a significant increase in systemic lethality compared to the wild type (Fig. 3C). These data suggest that EI is important in controlling virulence at the site of localized skin infections, as well as potentially serving a CovS-dependent role in limiting dissemination to sterile sites of the body.

The Δ*ptsI* mutant increases secretion of SpeB in a strain-specific manner. The cysteine protease SpeB is a well-characterized

TABLE 3 Growth of the wild-type MGAS5005 strain and MGAS5005.Δ*ptsI* mutant strain on various carbon sources by Biolog

Carbon source[a]	Metabolism[b] by the following strain on the indicated carbon source:	
	MGAS5005	MGAS5005.Δ*ptsI*
D-Galactose	+	−
D-Trehalose	+	−
D-Fructose	+	−
D-Mannose	+	−
α-D-Lactose	+	−
Sucrose	+	−
Maltotriose	+	−
Salicin	+	−
β-Methyl-D-glucoside	+	−
L-Lactic acid	+/−	−
D-Glucose-6-phosphate	+/−	−
Thymidine	+	−
Lactulose	+/−	−
D-Fructose-6-phosphate	+	−
N-Acetyl-β-D-mannosamine	+	−
α-Cyclodextrin	+	−
β-Cyclodextrin	+/−	−
5-Keto-D-gluconic acid	+	−
Glycerol	+	−
L-Arabinose	+	+
N-Acetyl-D-glucosamine	+	+
D-Xylose	+	+
D-Ribose	+	+
α-D-Glucose	+	+
Maltose	+	+
Uridine	+	+
Adenosine	+	+
Inosine	+	+
L-Lyxose	+	+
Pyruvic acid	+	+
Dextrin	+	+
Glycogen	+	+
β-D-Allose	+	+
D-Arabinose	+	+
2-Deoxy-D-ribose	+	+
D-Fucose	+	+
3-*O*-β-D-Galactopyranosyl-D-arabinose	+	+
3-*methyl*-Glucose	+	+
Palatinose	+	+
L-Sorbose	+	+
D-Tagatose	+	+
Turanose	+	+
D-Glucosamine	+	+
Oxalomalic acid	+	+
Dihydroxyacetone	+	+

[a] PTS sugars are indicated in boldface type.
[b] Symbols: +, metabolism of more than twofold the background level; −, metabolism not over twofold the background level; +/−, metabolism twofold the background level.

secreted virulence factor that has been shown to be a key contributor in various models of GAS skin infection, including ulcerative lesion formation (34–36). To investigate whether the M1T1 Δ*ptsI* mutants resulted in altered *speB* transcript levels, quantitative RT-PCR (qRT-PCR) was performed on mRNA isolated from the wild type and the corresponding isogenic Δ*ptsI* mutant from all three M1T1 strains at the transition phase of growth. No significant differences (greater than 2-fold) in *speB* transcript levels were observed for any of the three Δ*ptsI* mutants compared to their respective parental strain (data not shown), suggesting that transcription of *speB* is not altered in any of the mutants.

Increased secretion of active SpeB by GAS has been shown to negatively affect the formation of biofilms (36–38) and can be used as an indirect reporter for SpeB activity. A biofilm formation assay (see Supplemental Methods in the supplemental material) was performed on each M1T1 wild type and its respective Δ*ptsI* mutant. Cells were grown in a 6-well plate and allowed to grow for 24 h at 37°C, and biofilm formation was quantified by crystal violet staining. The MGAS5005.Δ*ptsI* and 5448AP.Δ*ptsI* strains, both with *covS* mutant backgrounds, showed significantly less biofilm than their wild-type parental strains (Fig. S2A to S2C, left). Importantly, the reduction seen in these Δ*ptsI* mutants could be reversed with the addition of the cysteine protease inhibitor E64 (Fig. S2A to S2C, left). In contrast, 5448.Δ*ptsI* showed no significant difference compared to the wild-type 5448. It should be noted that 5448 showed reduced ability to form biofilm compared to MGAS5005 and 5448AP, and an MGAS5005.Δ*spe*B control exhibited no significance difference in biofilm formation compared to MGAS5005 (Fig. S2A).

Secretion of SpeB into the supernatants from all three Δ*ptsI* mutants and their wild-type strains was assayed by Western blotting using a polyclonal SpeB antibody. No differences were observed in the amount of cell-bound SpeB of Δ*ptsI* mutants compared with their corresponding wild-type strain (data not shown). However, dramatically increased levels of secreted SpeB (both 40-kDa zymogen and 28-kDa mature forms) were detected in the culture supernatants from the MGAS5005.Δ*ptsI* and 5448AP.Δ*ptsI* mutant strains compared to their isogenic *covS* parental strains (see Fig. S2A to S2C, right, in the supplemental material). Interestingly, 5448.Δ*ptsI* had decreased levels of secreted SpeB compared to wild-type 5448, which correlates with the ability to form biofilm. Although this strongly suggests that EI (PTS) may reduce SpeB secretion in a CovS-dependent manner (MGAS5005Δ*ptsI* and 5448APΔ*ptsI*), this does not provide a mechanism for how increased lesion severity occurs in 5448.Δ*ptsI*.

Δ*ptsI* mutants exhibit expression of SLS during log-phase growth. Streptolysin S (SLS) is a secreted virulence factor that contributes to the formation of lesions in soft tissue models of mouse infection and GAS virulence in general (34, 39, 40). Biosynthesis and secretion of SLS in GAS require the 9-gene *sag* operon, with *sagA* encoding the toxin precursor and the first position in the locus (41). To determine whether the Δ*ptsI* mutation affects *sag* operon expression, qRT-PCR was performed on the isolated mRNA of the MGAS5005 strain, MGAS5005.Δ*ptsI* mutant, and the complemented MGAS5005.Δ*ptsI*c to quantify *sagA* transcript levels in late-log-phase cells in THY. Changes in transcript levels greater than 2-fold were considered significant. A modest yet significant increase in *sagA* transcript levels was observed in the Δ*ptsI* mutants compared to their corresponding wild-type strains (Fig. 4A to C) at this time point.

SLS-specific hemolytic activity was assayed using 2.5% defibrinated sheep RBCs incubated with culture supernatants from the wild-type MGAS5005 and mutant MGAS5005.Δ*ptsI* GAS taken at 1-h intervals across growth. Addition of the SLS inhibitor trypan blue blocked all RBC lysis in each experiment, indicating that the observed hemolytic activity was due to SLS (data not shown). SLS hemolytic activity in the MGAS5005.Δ*ptsI* mutant supernatants showed a dramatic increase early in logarithmic

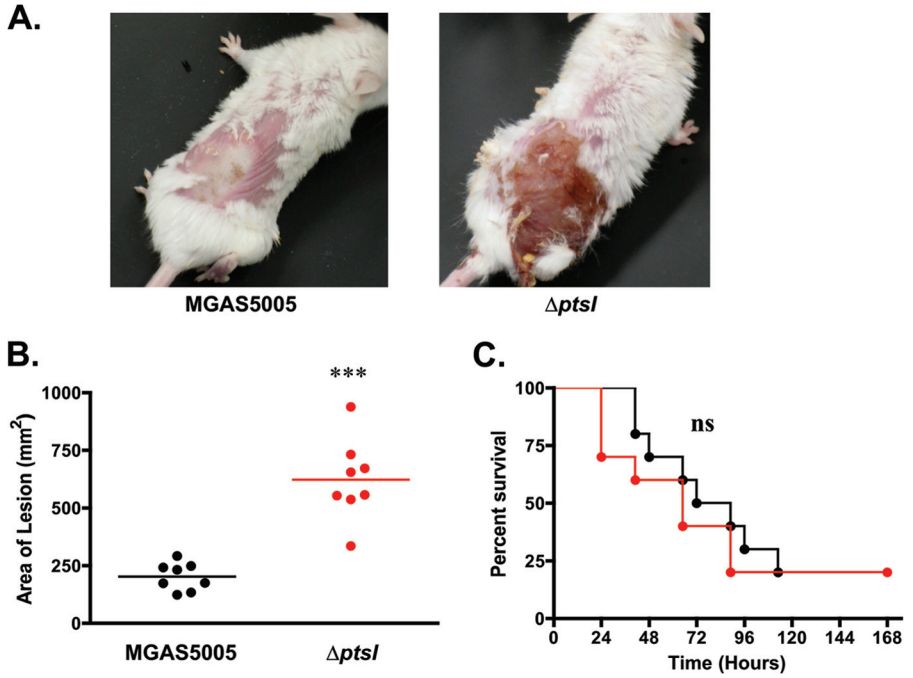

FIG 2 Effect of M1T1 MGAS5005.Δ*ptsI* mutant in mouse model of GAS infection. Mice were inoculated s.c. with ~3×10^8 CFU and monitored for 7 days. (A) Representative images of mice infected with wild-type MGAS5005 or the Δ*ptsI* mutant at 38 h postinfection. (B) Lesion sizes measured in mice infected with the MGAS5005 strain (black) and Δ*ptsI* mutant (red) at 38 h postinfection. One of two independent experiments is shown (the total number of mice was 40). Each symbol represents the value for a single animal, and the horizontal bars indicate the mean value for the group. Statistical significance was determined by unpaired two-tailed *t* test of the animals shown. (C) Survival plot of mice infected with MGAS5005 or its Δ*ptsI* mutant over the course of 7 days. Significance was determined by Kaplan-Meier survival analysis and log rank test of the animals shown (***, $P \leq 0.001$; ns, not significant).

phase and remained elevated during stationary phase (Fig. 4D). In comparison, SLS hemolytic activity from the supernatants of the wild type and the complemented Δ*ptsI* strain showed little activity during logarithmic phase and increased to maximum levels at the transition to stationary phase (Fig. 4D), as previously observed for SLS (19). Similarly, an early onset of SLS hemolytic activity was observed for the 5448.Δ*ptsI* and 5448AP.Δ*ptsI* mutants in comparison to their respective wild-type strains (Fig. 4E and F). These data suggest that the early onset of SLS activity during exponential-phase growth in all three M1T1 GAS strains lacking a functional PTS could lead to the increased severity of localized lesions observed in mice (Fig. 2 and 3).

SLS is required for the lesion severity observed in M1T1 Δ*ptsI* mutants. The role of SLS in the hypervirulence of lesions of mice infected with Δ*ptsI* mutants was investigated by creating a Δ*ptsI sagB* double mutant from the MGAS5005 strain. Inactivation of *sagB* has been shown to block SLS production in M1T1 GAS (19, 41). As expected, a Δ*ptsI sagB* double mutant resulted in the absence of hemolytic activity both on blood agar plates (Fig. 5A) and also in RBC hemolysis assays (data not shown) comparable to an established MGAS5005.*sagB* mutant (Fig. 5) (19). To investigate the role of SLS *in vivo*, MGAS5005, MGAS5005.Δ*ptsI*, MGAS5005.Δ*sagB*, and the MGAS5005.Δ*ptsI sagB* double mutant were tested in the murine model of streptococcal soft tissue infection (Fig. 5B and C). The nonhemolytic Δ*sagB* mutant (19) showed lesion sizes comparable to those of the wild-type MGAS5005 (Fig. 5C), indicating that SLS does not normally contribute significantly to ulcer formation in this M1T1 background at the time point observed. Despite the absence of a functional PTS, the Δ*ptsI sagB* double mutant lacking expression of SLS produced purulent lesions with a size and severity comparable to those of the wild type and Δ*sagB* strains, and not the Δ*ptsI* mutant (Fig. 5B and C). These results strongly suggest that altered temporal expression of SLS during growth is the primary factor responsible for the increased lesion size and severity observed upon subcutaneous infection of mice with the Δ*ptsI* mutant.

DISCUSSION

Although the connections between carbon metabolism and pathogenesis in GAS have been recognized for many years, the contribution of the PTS pathway to GAS virulence has yet to be investigated. In this study, we generated PTS mutants from multiple strains of GAS by deleting *ptsI* (EI) and characterized their growth profiles to identify the PTS-dependent carbon sources that support the growth of M1T1 GAS *in vitro*. Importantly, a PTS mutant was still able to colonize and elicit disease in a murine model of disseminating soft tissue infection. However, the PTS mutant resulted in a significant increase in localized lesion severity and size due to an increase in *sag* operon expression and an altered temporal expression of streptolysin S (SLS). Thus, a functional PTS appears to limit the pathogenesis of GAS during invasive skin infection.

PTS pathway and carbon utilization in GAS. The PTS carbohydrate transport system is widespread in bacteria, where it shares the same basic composition in all genera; two "general" cytoplasmic components, EI and HPr, and sugar-specific EII transporters located in the cytoplasmic membrane (10). Typically, the genes encoding Hpr (*ptsH*) and EI (*ptsI*) are organized as a tightly regu-

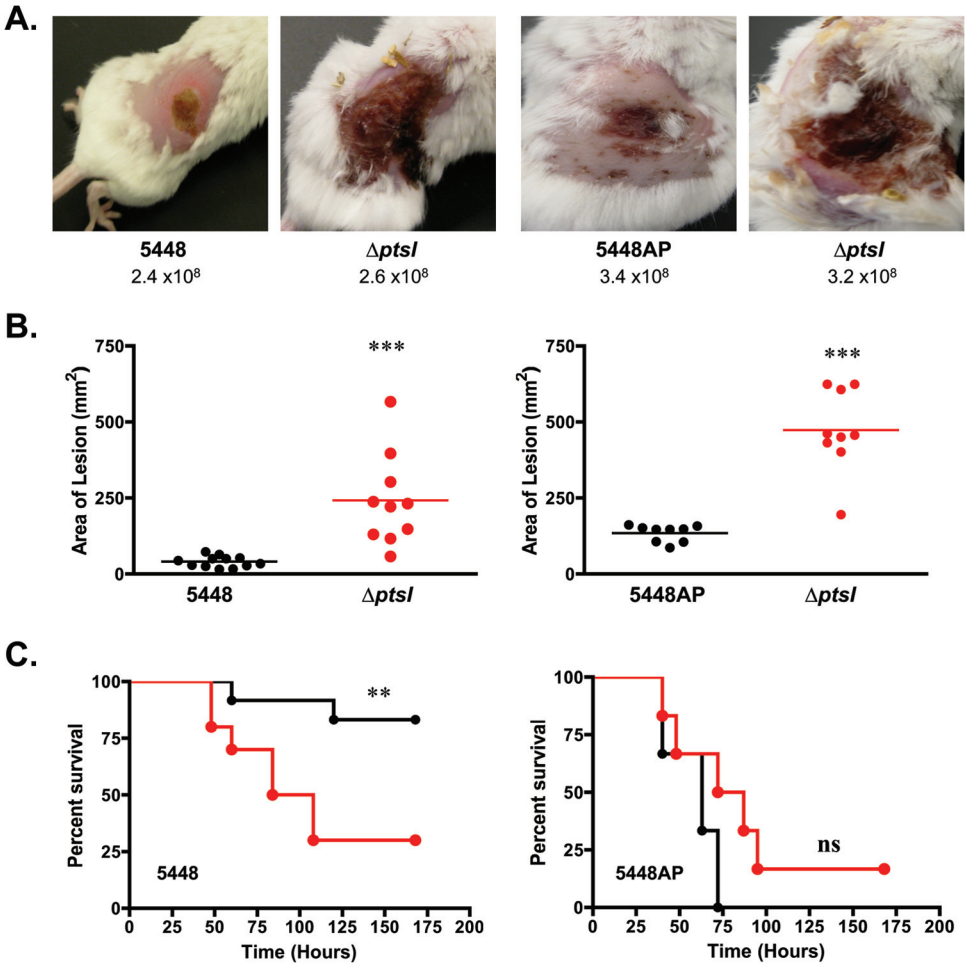

FIG 3 Δ*ptsI* mutants of additional M1T1 GAS strains. (A) Representative images of mice infected s.c. with strain 5448 (CovS$^+$) and its Δ*ptsI* mutant (left) or 5448AP (CovS$^-$) and its Δ*ptsI* mutant (right) at 38 h postinfection. The numbers of CFU used in infection are indicated. (B) Lesion sizes of the same strains measured at 38 h postinfection from a representative experiment (the total number of mice is 60). Each symbol represents the value for a single animal, with the horizontal bars indicating the mean values for groups. Statistical significance was determined by unpaired two-tailed *t* test. (C) Survival plot of mice infected with either wild-type 5448 and 5448AP in black and their corresponding Δ*ptsI* mutants in red. Significance was determined by Kaplan-Meier survival analysis and log rank test (**, $P \leq 0.01$; ***, $P \leq 0.001$; NS, not significant).

lated *ptsHI* operon (42), and this appears to be the case for GAS as well. Several attempts to construct either a nonpolar deletion or a polar insertion mutation of *ptsH* were unsuccessful (data not shown), suggesting that Hpr may be critical for GAS fitness under the conditions used here. This observation has been further supported by Tn-Seq essentiality studies ongoing in our lab (Y. Le Breton and K. S. McIver, unpublished results). Our results also confirm work done in closely related streptococci, such as *S. pneumoniae* (43) and *S. mutans* (23), as well as *Staphylococcus aureus* (44, 45) and *Mycoplasma* species (46, 47), where *ptsH* (Hpr) has also been reported to be essential for growth. In contrast to *ptsH*, we were able to generate a nonpolar *ptsI* (EI) deletion mutant in 3 different strains of M1T1 GAS and in an M4 GAS strain (3), indicating that the PTS itself is not required and that Hpr appears to possess a separate essential function in GAS. Despite being able to make *ptsI* null mutations in GAS, attempts to clone *ptsI* on a multicopy plasmid for complementation proved to be difficult, and we were successful only when the construct lacked a functional promoter. This suggests that overexpression of *ptsI* can be deleterious in *E. coli* and that the *ptsHI* operon is likely under tight regulation in GAS.

By screening with the Biolog phenotypic microarray platform, we established that 45 of 190 carbon sources tested were able to support the metabolism (defined as 2-fold over background) of the M1T1 GAS invasive throat strain MGAS5005 (Table 3). In contrast, Siemens et al. identified only 21 carbon sources with Biolog that supported the metabolism (defined as ≥10% of metabolism on glucose) of the M49 GAS "generalist" strain 591, a strain that is able to colonize both the throat and skin (48). Out of these 21 carbon sources, all but 5 (Tween 40, Tween 80, pectin, mannan, and gelatin) were in common with our studies in M1T1 (Table 3). The different metrics used to determine functional growth in the two studies could explain some of the disparity in carbon sources. However, it could also indicate that metabolic requirements differ between strains of GAS, likely due to their varied tissue sites of infection. *S. pneumoniae*, which is found primarily in the nasopharynx, can utilize 29 different carbon sources in Biolog, 16 of which overlapped with our M1T1 GAS findings

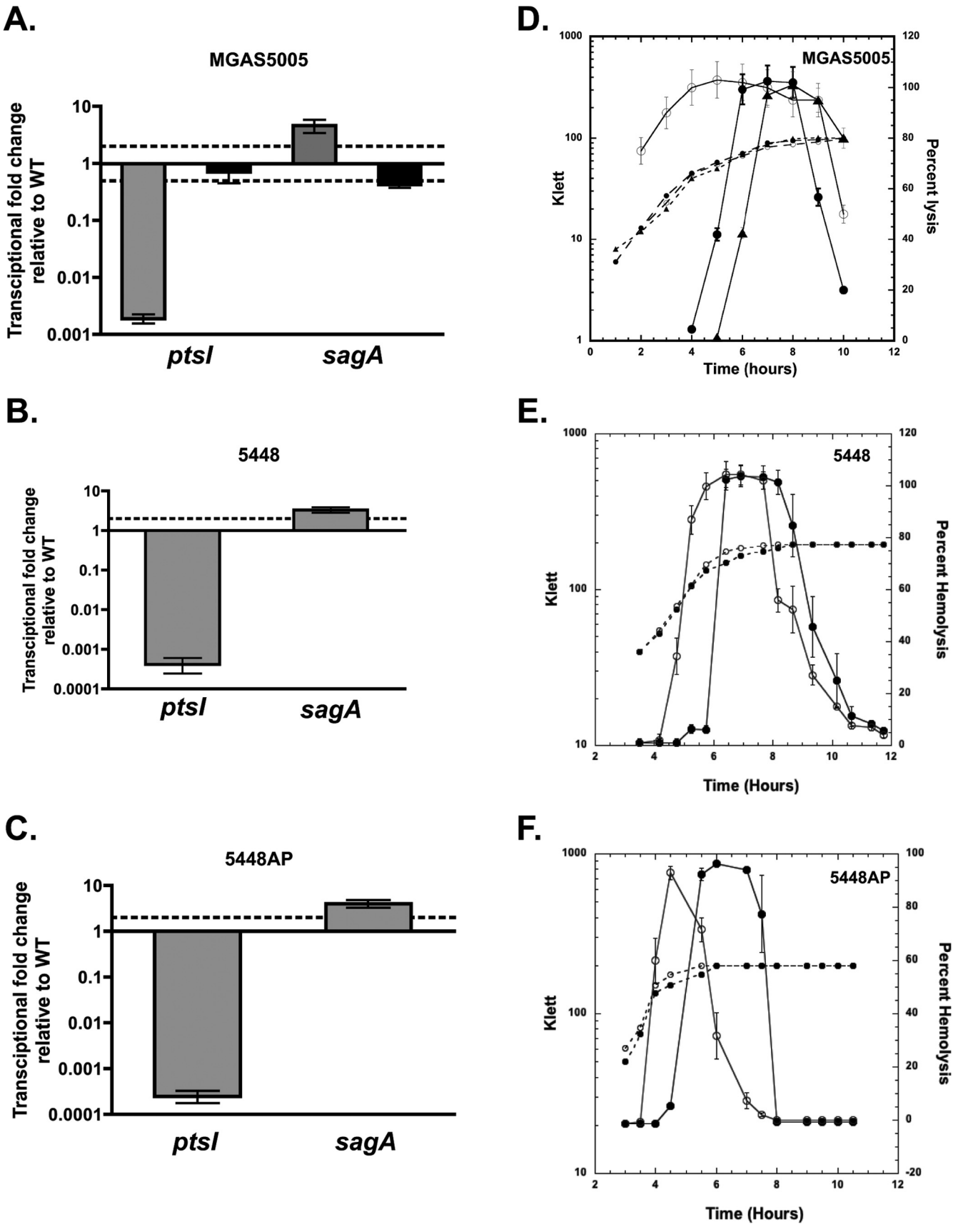
A.
MGAS5005
Transciptional fold change relative to WT
10
1
0.1
0.01
0.001
ptsI
sagA
B.
5448
Transciptional fold change relative to WT
10
1
0.1
0.01
0.001
0.0001
ptsI
sagA
C.
5448AP
Transciptional fold change relative to WT
10
1
0.1
0.01
0.001
0.0001
ptsI
sagA
D.
MGAS5005
Klett
Percent lysis
Time (hours)
E.
5448
Klett
Percent Hemolysis
Time (Hours)
F.
5448AP
Klett
Percent Hemolysis
Time (Hours)

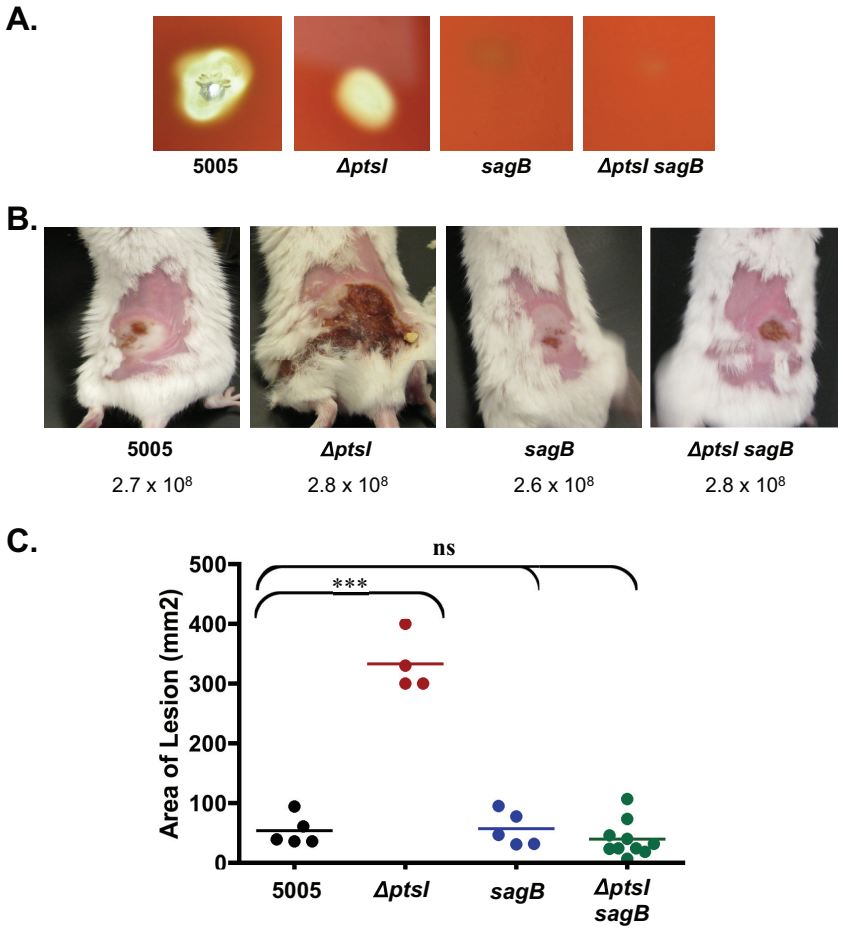

FIG 5 Role of streptolysin S in Δ*ptsI* increased lesion formation. (A) Zones of hemolysis for wild-type (WT) MGAS5005, Δ*ptsI* single mutant, Δ*sagB* single mutant, and Δ*sagB* Δ*ptsI* double mutant strains on 5% sheep blood agar plates after growth at 37°C. (B) Representative images of mice infected s.c. with WT MGAS5005, MGAS5005.Δ*ptsI* mutant, Δ*sagB* single mutant, and Δ*ptsI sagB* double mutant strains. The numbers of CFU used in infection are indicated. (C) Lesion size of the same experiment measured at 38 h after s.c. infection of MGAS5005 (black), Δ*ptsI* mutant (red), Δ*sagB* mutant (blue), and Δ*ptsI sagB* double mutant (green). Data represent two independent experiments, and significance was determined using the unpaired two-tailed *t* test (***, $P \leq 0.001$; ns, not significant).

(Table 3). Thus, many of the carbon sources are similar for streptococci; however, they appear to possess niche- and species-specific requirements.

The M1T1 MGAS5005 GAS genome possesses 14 putative EII loci (49) predicted for the transport of specific PTS sugars, although the exact substrates transported by most of these systems have not been experimentally determined. The isogenic Δ*ptsI* M1T1 MGAS5005 mutant was still able to utilize 26 of the 45 carbon sources required for wild-type metabolism (Table 3), indicating that GAS does not need a functional PTS to utilize these carbon sources. However, the Δ*ptsI* mutant did show metabolic defects with 19 carbon sources (Table 3), including 8 predicted PTS-specific carbohydrates (galactose, trehalose, fructose, mannose, lactose, sucrose, salicin, and maltotriose). Growth defects on maltose and glucose were not found in our study likely due to the presence of non-PTS uptake systems. Transport of maltose in GAS has been shown to occur through both the MalE-dependent ABC transport system as well as the MalT-specific PTS pathway (49, 50). In *Lactococcus lactis*, a non-PTS glucose uptake system (GlcU) has been reported; however, genes encoding a homologous system have not yet been identified in the genomes of *S. pyogenes* or *S. pneumoniae* (51). Interestingly, there is a putative glucokinase gene present in the MGAS5005 genome that could act to phosphorylate glucose uptake via a non-PTS transport system. The

FIG 4 Influence of Δ*ptsI* on streptolysin S (SLS) production. (A to C) Transcript levels of *sagA* were measured by qRT-PCR at late log phase in THY for the wild type (WT) and the complemented MGAS5005.Δ*ptsI*c strain and isogenic *ptsI* mutants of strains MGAS5005 (A), 5448 (B), and 5448AP (C). Twofold differences in expression for mutant compared to the wild type (dashed line) were considered significant. (D to F) SLS hemolytic activity was measured in culture supernatants for the wild type (closed circles) and isogenic *ptsI* mutants (open circles) of strains MGAS5005 (D), 5448 (E), and 5448AP (F) and the complemented Δ*ptsI* mutant (closed triangles). Strains were grown in THY supplemented with 10% heat-inactivated horse serum and supernatants isolated throughout growth for analysis of SLS activity. Data are presented as percent hemolysis (solid lines) for three biological replicates. Representative growth curves for the strains are shown as dashed lines.

identity of the non-PTS glucose transporter in GAS remains to be determined. In addition to the six carbon compounds, Δ*ptsI* blocked the utilization of α-glucosides (trehalose, sucrose, and maltotriose), β-galactosides (lactose and lactulose), β-glucosides (β-methyl-D-glucoside and salicin), cyclodextrins, lactic acid, and the three-carbon compound glycerol (Table 3). The defect in the use of non-PTS glycerol can be explained by the fact that glycerol kinase of *Firmicutes* is phosphorylated by PEP, EI, and HPr and that this modification is necessary for the activation of the enzyme (52). The results suggest that the PTS plays a broader role in regulating PTS-dependent and non-PTS-dependent transport, as well as the subsequent utilization of these substrates in central carbon metabolism.

PTS limits lesion severity during invasive skin infection in mice. Despite the inability to utilize 19 PTS and non-PTS sugars (Table 3), all three independent M1T1 Δ*ptsI* mutants were able to colonize mice following subcutaneous inoculation and elicit both localized and systemic disease to at least the levels of the parental wild-type strains. This provides strong evidence that GAS does not require a functional PTS or these specific sugars to infect at this tissue site and likely utilizes a carbon source that is not altered in the Δ*ptsI* mutant (Table 3). In fact, lesion formation was significantly more rapid with increased necrosis and size in mice infected with mutant strains (Fig. 2, 3, and 5). Furthermore, mice infected by *ptsI* mutants exhibited highly ulcerative and spreading lesions that resulted in severe hemorrhaging and tissue damage. This is in sharp contrast to the phenotype of a Δ*ptsI* mutant in *Staphylococcus aureus*, where virulence was attenuated compared to the wild type in an intraperitoneal (i.p.) model of systemic infection in BALB/c mice (53). The difference may merely reflect the different site of infections. Regardless, a functional PTS acts to limit localized tissue damage in GAS during invasive skin infection, and this appears to be linked to the metabolism of sugars that require PTS transport (Table 3).

Dissemination of GAS from the subcutaneous site of infection to the bloodstream and organs leading to lethality was not significantly altered in the MGAS5005.Δ*ptsI* and 5448AP.Δ*ptsI* mutant strains compared to their parental strains (Fig. 2C and 3C). Both of these M1T1 strains possess a mutation in the *covS* histidine kinase gene that is associated with a molecular switch to a highly invasive phenotype for GAS. In contrast, deletion of *ptsI* in the M1T1 strain 5448 harboring a wild-type *covS* gene exhibited a significant increase in systemic lethality due to dissemination (Fig. 3C) that correlated with the increase in lesion severity observed in all of the mutants. Thus, there might be a Cov-dependent influence on the ability of a functional PTS to limit systemic spread as well as localized lesion formation, although other genetic differences unlinked to *cov* could be involved. At this point, we do not know which Cov-regulated factor(s) may be involved in this dissemination phenotype. The cysteine protease SpeB is regulated by Cov and has been directly associated with the formation of severe lesions in skin models of GAS infection (34–36). We observed a PTS-dependent regulation on secretion of SpeB, but it was not common to all three M1T1 backgrounds regardless of Cov status (see Fig. S2 in the supplemental material).

PTS represses *sag* expression and early SLS production. As mentioned above, the cytolysin SLS has been shown to contribute to the severity of skin lesions during GAS infection in mice (34, 39, 40). A modest upregulation of *sagA* at late log phase and increased SLS activity in the supernatants of the M1T1 Δ*ptsI* mutants early in growth correlates nicely with the rapid onset of ulcerative lesions observed in the mice infected with the mutants. Importantly, inactivating *sagB* (an SLS-defective mutant) in the MGAS5005.Δ*ptsI* background reversed this phenotype and resulted in localized lesions comparable to the lesions caused by the wild-type parental strain alone (Fig. 5). These data strongly suggest that early expression of SLS during growth is likely the primary factor responsible for the increased lesion size and severity observed upon subcutaneous infection of mice with the MGAS5005.Δ*ptsI* mutant and other M1T1 strains. Despite the absence of SLS hemolytic activity in the Δ*ptsI sagB* double mutant, lesion formation comparable to that of the wild type was still observed (Fig. 5). These results suggest that other virulence factors besides SLS are contributing to the lesion development seen in the parental M1T1 MGAS5005 strain.

A similar hypervirulent lesion phenotype, albeit not as significant, was previously observed by our group when a Δ*ccpA* mutant derived from the MGAS5005 strain was tested in the murine skin infection model. Importantly, this phenotype was attributed to CcpA-dependent overproduction of *sagA* and SLS (19). Other studies have actually found attenuation in virulence upon infection with a Δ*ccpA* mutant in M1T1 MGAS5005 and other GAS strains (18, 21). However, all studies observed an upregulation in *sag* operon transcription leading to increased SLS production in the mutants *in vitro*. Kietzman and Caparon showed that CcpA regulation of the *sag* operon in the M14 GAS strain HSC5 was indirect and that the repression did not appear to occur in infected skin tissue (18). The mechanism of indirect regulation of *sag* by CcpA has not been determined. Overall, this indicated that the absence of CCR in GAS modulates the regulation of SLS, but this appears to vary in strains. Since the CCR pathway remains intact in our Δ*ptsI* mutants (Hpr kinase, Hpr, and CcpA), our findings may reflect a novel pathway for influencing *sag* expression and SLS production based on carbohydrate availability. However, we cannot rule out the possibility that both CcpA and the PTS pathways are impinging indirectly on the same regulatory pathway and leading to repression of SLS production.

In addition to CcpA, the expression of *sagA* is under the transcriptional control of GAS global regulators such as CovRS, Mga, RofA, FasBCA, and Nra (54). Our study suggests the effect of *ptsI* on SLS activity is CovS independent; yet, there is published evidence that CovR regulates the *sag* operon by direct binding to the P*sagA* promoter (55). Thus, although we think that CovS is not involved, we cannot rule out a role for CovR. Other known regulators of the *sag* operon include the newly described PTS regulatory domain (PRD)-containing virulence regulators (PCVR) such as Mga and RofA (3). Thus, it is possible that signaling through PTS might influence the expression of global regulatory networks to influence the expression of SLS and other virulence factors in GAS.

In conclusion, we have used PTS-defective strains of M1T1 GAS to identify the PTS and non-PTS carbon sources that allow these invasive isolates to grow *in vitro*. The Δ*ptsI* mutants exhibited more severe and larger ulcerative lesions at the site of infection in a subcutaneous model of mouse infection. This phenotype was linked to upregulation of *sagA* and early onset of streptolysin S activity during exponential-phase growth in the mutant. Infection of mice with a Δ*ptsI sagB* double mutant returned lesions to wild-type levels, implicating SLS in the observed phenotype. Therefore, a functional PTS is not required for subcutaneous skin

infection in mice; however, it does limit early expression of SLS and thus the overall severity of lesions *in vivo*.

ACKNOWLEDGMENTS

We thank Yoann Le Breton, Surya Sundar, and Kayla Valdes for critical review of the manuscript.

This work was supported by a grant from the NIH National Institute of Allergy and Infectious Diseases (AI047928) to K.S.M.

REFERENCES

1. **Deutscher J, Francke C, Postma PW.** 2006. How phosphotransferase system-related protein phosphorylation regulates carbohydrate metabolism in bacteria. Microbiol. Mol. Biol. Rev. **70:**939–1031. http://dx.doi.org/10.1128/MMBR.00024-06.
2. **Gorke B, Stulke J.** 2008. Carbon catabolite repression in bacteria: many ways to make the most out of nutrients. Nat. Rev. Microbiol. **6:**613–624. http://dx.doi.org/10.1038/nrmicro1932.
3. **Hondorp ER, Hou SC, Hause LL, Gera K, Lee CE, McIver KS.** 2013. PTS phosphorylation of Mga modulates regulon expression and virulence in the group A streptococcus. Mol. Microbiol. **88:**1176–1193. http://dx.doi.org/10.1111/mmi.12250.
4. **Cho KH, Caparon MG.** 2005. Patterns of virulence gene expression differ between biofilm and tissue communities of *Streptococcus pyogenes*. Mol. Microbiol. **57:**1545–1556. http://dx.doi.org/10.1111/j.1365-2958.2005.04786.x.
5. **Munoz-Elias EJ, McKinney JD.** 2005. *Mycobacterium tuberculosis* isocitrate lyases 1 and 2 are jointly required for in vivo growth and virulence. Nat. Med. **11:**638–644. http://dx.doi.org/10.1038/nm1252.
6. **Rollenhagen C, Bumann D.** 2006. *Salmonella enterica* highly expressed genes are disease specific. Infect. Immun. **74:**1649–1660. http://dx.doi.org/10.1128/IAI.74.3.1649-1660.2006.
7. **Iyer R, Camilli A.** 2007. Sucrose metabolism contributes to *in vivo* fitness of Streptococcus pneumoniae. Mol. Microbiol. **66:**1–13. http://dx.doi.org/10.1111/j.1365-2958.2007.05878.x.
8. **Son MS, Matthews WJ, Jr, Kang Y, Nguyen DT, Hoang TT.** 2007. In vivo evidence of *Pseudomonas aeruginosa* nutrient acquisition and pathogenesis in the lungs of cystic fibrosis patients. Infect. Immun. **75:**5313–5324. http://dx.doi.org/10.1128/IAI.01807-06.
9. **Lengeler JW, Jahreis K.** 2009. Bacterial PEP-dependent carbohydrate: phosphotransferase systems couple sensing and global control mechanisms. Contrib. Microbiol. **16:**65–87. http://dx.doi.org/10.1159/000219373.
10. **Postma PW, Lengeler JW, Jacobson GR.** 1993. Phosphoenolpyruvate: carbohydrate phosphotransferase systems of bacteria. Microbiol. Rev. **57:**543–594.
11. **Kruger S, Gertz S, Hecker M.** 1996. Transcriptional analysis of bglPH expression in *Bacillus subtilis*: evidence for two distinct pathways mediating carbon catabolite repression. J. Bacteriol. **178:**2637–2644.
12. **McAllister LJ, Ogunniyi AD, Stroeher UH, Paton JC.** 2012. Contribution of a genomic accessory region encoding a putative cellobiose phosphotransferase system to virulence of *Streptococcus pneumoniae*. PLoS One **7:**e32385. http://dx.doi.org/10.1371/journal.pone.0032385.
13. **Antunes A, Martin-Verstraete I, Dupuy B.** 2011. CcpA-mediated repression of *Clostridium difficile* toxin gene expression. Mol. Microbiol. **79:**882–899. http://dx.doi.org/10.1111/j.1365-2958.2010.07495.x.
14. **Stoll R, Mertins S, Joseph B, Muller-Altrock S, Goebel W.** 2008. Modulation of PrfA activity in *Listeria monocytogenes* upon growth in different culture media. Microbiology **154:**3856–3876. http://dx.doi.org/10.1099/mic.0.2008/018283-0.
15. **Tsvetanova B, Wilson AC, Bongiorni C, Chiang C, Hoch JA, Perego M.** 2007. Opposing effects of histidine phosphorylation regulate the AtxA virulence transcription factor in *Bacillus anthracis*. Mol. Microbiol. **63:**644–655.
16. **Fujita Y.** 2009. Carbon catabolite control of the metabolic network in *Bacillus subtilis*. Biosci. Biotechnol. Biochem. **73:**245–259. http://dx.doi.org/10.1271/bbb.80479.
17. **Iyer R, Baliga NS, Camilli A.** 2005. Catabolite control protein A (CcpA) contributes to virulence and regulation of sugar metabolism in *Streptococcus pneumoniae*. J. Bacteriol. **187:**8340–8349. http://dx.doi.org/10.1128/JB.187.24.8340-8349.2005.
18. **Kietzman CC, Caparon MG.** 2010. CcpA and LacD.1 affect temporal regulation of *Streptococcus pyogenes* virulence genes. Infect. Immun. **78:**241–252. http://dx.doi.org/10.1128/IAI.00746-09.
19. **Kinkel TL, McIver KS.** 2008. CcpA-mediated repression of streptolysin S expression and virulence in the group A streptococcus. Infect. Immun. **76:**3451–3463. http://dx.doi.org/10.1128/IAI.00343-08.
20. **Seidl K, Stucki M, Ruegg M, Goerke C, Wolz C, Harris L, Berger-Bachi B, Bischoff M.** 2006. *Staphylococcus aureus* CcpA affects virulence determinant production and antibiotic resistance. Antimicrob. Agents Chemother. **50:**1183–1194. http://dx.doi.org/10.1128/AAC.50.4.1183-1194.2006.
21. **Shelburne SA, III, Keith D, Horstmann N, Sumby P, Davenport MT, Graviss EA, Brennan RG, Musser JM.** 2008. A direct link between carbohydrate utilization and virulence in the major human pathogen group A *Streptococcus*. Proc. Natl. Acad. Sci. U. S. A. **105:**1698–1703. http://dx.doi.org/10.1073/pnas.0711767105.
22. **Varga J, Stirewalt VL, Melville SB.** 2004. The CcpA protein is necessary for efficient sporulation and enterotoxin gene (*cpe*) regulation in *Clostridium perfringens*. J. Bacteriol. **186:**5221–5229. http://dx.doi.org/10.1128/JB.186.16.5221-5229.2004.
23. **Zeng L, Burne RA.** 2010. Seryl-phosphorylated HPr regulates CcpA-independent carbon catabolite repression in conjunction with PTS permeases in *Streptococcus mutans*. Mol. Microbiol. **75:**1145–1158. http://dx.doi.org/10.1111/j.1365-2958.2009.07029.x.
24. **Carapetis JR, Steer AC, Mulholland EK, Weber M.** 2005. The global burden of group A streptococcal diseases. J. Gen. Microbiol. **129:**643–651. http://dx.doi.org/10.1099/00221287-129-3-643.
25. **Dassy B, Alouf JE.** 1983. Growth of *Streptococcus pyogenes* and streptolysin O production in complex and synthetic media. J. Gen. Microbiol. **129:**643–651. http://dx.doi.org/10.1099/00221287-129-3-643.
26. **Pine L, Reeves MW.** 1978. Regulation of the synthesis of M protein by sugars, Todd Hewitt broth, and horse serum, in growing cells of *Streptococcus pyogenes*. Microbios **21:**185–212.
27. **Musser JM, Shelburne SA, III.** 2009. A decade of molecular pathogenomic analysis of group A Streptococcus. J. Clin. Invest. **119:**2455–2463. http://dx.doi.org/10.1172/JCI38095.
28. **Loughman JA, Caparon MG.** 2006. A novel adaptation of aldolase regulates virulence in *Streptococcus pyogenes*. EMBO J. **25:**5414–5422. http://dx.doi.org/10.1038/sj.emboj.7601393.
29. **Sumby P, Porcella SF, Madrigal AG, Barbian KD, Virtaneva K, Ricklefs SM, Sturdevant DE, Graham MR, Vuopio-Varkila J, Hoe NP, Musser JM.** 2005. Evolutionary origin and emergence of a highly successful clone of serotype M1 group A Streptococcus involved multiple horizontal gene transfer events. J. Infect. Dis. **192:**771–782. http://dx.doi.org/10.1086/432514.
30. **Podbielski A, Woischnik M, Kreikemeyer B, Bettenbrock K, Buttaro BA.** 1999. Cysteine protease SpeB expression in group A streptococci is influenced by the nutritional environment but SpeB does not contribute to obtaining essential nutrients. Med. Microbiol. Immunol. **188:**99–109. http://dx.doi.org/10.1007/s004300050111.
31. **van de Rijn I, Kessler RE.** 1980. Growth characteristics of group A streptococci in a new chemically defined medium. Infect. Immun. **27:**444–448.
32. **Horton RM.** 1995. PCR-mediated recombination and mutagenesis. SOEing together tailor-made genes. Mol. Biotechnol. **3:**93–99.
33. **Lukomski S, Hoe NP, Abdi I, Rurangirwa J, Kordari P, Liu M, Dou SJ, Adams GG, Musser JM.** 2000. Nonpolar inactivation of the hypervariable streptococcal inhibitor of complement gene (*sic*) in serotype M1 *Streptococcus pyogenes* significantly decreases mouse mucosal colonization. Infect. Immun. **68:**535–542. http://dx.doi.org/10.1128/IAI.68.2.535-542.2000.
34. **Engleberg NC, Heath A, Vardaman K, DiRita VJ.** 2004. Contribution of CsrR-regulated virulence factors to the progress and outcome of murine skin infections by *Streptococcus pyogenes*. Infect. Immun. **72:**623–628. http://dx.doi.org/10.1128/IAI.72.2.623-628.2004.
35. **Lukomski S, Montgomery CA, Rurangirwa J, Geske RS, Barrish JP, Adams GJ, Musser JM.** 1999. Extracellular cysteine protease produced by *Streptococcus pyogenes* participates in the pathogenesis of invasive skin infection and dissemination in mice. Infect. Immun. **67:**1779–1788.
36. **Connolly KL, Roberts AL, Holder RC, Reid SD.** 2011. Dispersal of group A streptococcal biofilms by the cysteine protease SpeB leads to increased disease severity in a murine model. PLoS One **6:**e18984. http://dx.doi.org/10.1371/journal.pone.0018984.
37. **Doern CD, Roberts AL, Hong W, Nelson J, Lukomski S, Swords WE,**

Reid SD. 2009. Biofilm formation by group A Streptococcus: a role for the streptococcal regulator of virulence (Srv) and streptococcal cysteine protease (SpeB). Microbiology **155:**46–52. http://dx.doi.org/10.1099/mic.0.021048-0.

38. **Roberts AL, Holder RC, Reid SD.** 2010. Allelic replacement of the streptococcal cysteine protease SpeB in a Δ*srv* mutant background restores biofilm formation. BMC Res. Notes **3:**281. http://dx.doi.org/10.1186/1756-0500-3-281.
39. **Fontaine MC, Lee JJ, Kehoe MA.** 2003. Combined contributions of streptolysin O and streptolysin S to virulence of serotype M5 *Streptococcus pyogenes* strain Manfredo. Infect. Immun. **71:**3857–3865. http://dx.doi.org/10.1128/IAI.71.7.3857-3865.2003.
40. **Heath A, DiRita VJ, Barg NL, Engleberg NC.** 1999. A two-component regulatory system, CsrR-CsrS, represses expression of three *Streptococcus pyogenes* virulence factors, hyaluronic acid capsule, streptolysin S, and pyrogenic exotoxin B. Infect. Immun. **67:**5298–5305.
41. **Nizet V, Beall B, Bast DJ, Datta V, Kilburn L, Low DE, De Azavedo JC.** 2000. Genetic locus for streptolysin S production by group A streptococcus. Infect. Immun. **68:**4245–4254. http://dx.doi.org/10.1128/IAI.68.7.4245-4254.2000.
42. **Vadeboncoeur C, Frenette M, Lortie LA.** 2000. Regulation of the *pts* operon in low G+C Gram-positive bacteria. J. Mol. Microbiol. Biotechnol. **2:**483–490.
43. **Song JH, Ko KS, Lee JY, Baek JY, Oh WS, Yoon HS, Jeong JY, Chun J.** 2005. Identification of essential genes in *Streptococcus pneumoniae* by allelic replacement mutagenesis. Mol. Cells **19:**365–374.
44. **Forsyth RA, Haselbeck RJ, Ohlsen KL, Yamamoto RT, Xu H, Trawick JD, Wall D, Wang L, Brown-Driver V, Froelich JM, Kedar GC, King P, McCarthy M, Malone C, Misiner B, Robbins D, Tan Z, Zhu ZY, Carr G, Mosca DA, Zamudio C, Foulkes JG, Zyskind JW.** 2002. A genome-wide strategy for the identification of essential genes in *Staphylococcus aureus*. Mol. Microbiol. **43:**1387–1400. http://dx.doi.org/10.1046/j.1365-2958.2002.02832.x.
45. **Chaudhuri RR, Allen AG, Owen PJ, Shalom G, Stone K, Harrison M, Burgis TA, Lockyer M, Garcia-Lara J, Foster SJ, Pleasance SJ, Peters SE, Maskell DJ, Charles IG.** 2009. Comprehensive identification of essential *Staphylococcus aureus* genes using Transposon-Mediated Differential Hybridisation (TMDH). BMC Genomics **10:**291. http://dx.doi.org/10.1186/1471-2164-10-291.
46. **Glass JI, Assad-Garcia N, Alperovich N, Yooseph S, Lewis MR, Maruf M, Hutchison CA, III, Smith HO, Venter JC.** 2006. Essential genes of a minimal bacterium. Proc. Natl. Acad. Sci. U. S. A. **103:**425–430. http://dx.doi.org/10.1073/pnas.0510013103.
47. **French CT, Lao P, Loraine AE, Matthews BT, Yu H, Dybvig K.** 2008. Large-scale transposon mutagenesis of *Mycoplasma pulmonis*. Mol. Microbiol. **69:**67–76. http://dx.doi.org/10.1111/j.1365-2958.2008.06262.x.
48. **Siemens N, Fiedler T, Normann J, Klein J, Munch R, Patenge N, Kreikemeyer B.** 2012. Effects of the ERES pathogenicity region regulator Ralp3 on *Streptococcus pyogenes* serotype M49 virulence factor expression. J. Bacteriol. **194:**3618–3626. http://dx.doi.org/10.1128/JB.00227-12.
49. **Shelburne SA, III, Keith DB, Davenport MT, Horstmann N, Brennan RG, Musser JM.** 2008. Molecular characterization of group A Streptococcus maltodextrin catabolism and its role in pharyngitis. Mol. Microbiol. **69:**436–452. http://dx.doi.org/10.1111/j.1365-2958.2008.06290.x.
50. **Shelburne SA, Fang H, Okorafor N, Sumby P, Stikiewicz I, Keith D, Patel P, Austin C, Graviss EA, Musser JM, Chow D.** 2007. MalE of group A *Streptococcus* participates in the rapid transport of maltotriose and longer maltodextrins. J. Bacteriol. **189:**2610–2617. http://dx.doi.org/10.1128/JB.01539-06.
51. **Bidossi A, Mulas L, Decorosi F, Colomba L, Ricci S, Pozzi G, Deutscher J, Viti C, Oggioni MR.** 2012. A functional genomics approach to establish the complement of carbohydrate transporters in *Streptococcus pneumoniae*. PLoS One **7:**e33320. http://dx.doi.org/10.1371/journal.pone.0033320.
52. **Darbon E, Servant P, Poncet S, Deutscher J.** 2002. Antitermination by GlpP, catabolite repression via CcpA and inducer exclusion triggered by P-GlpK dephosphorylation control *Bacillus subtilis* glpFK expression. Mol. Microbiol. **43:**1039–1052. http://dx.doi.org/10.1046/j.1365-2958.2002.02800.x.
53. **Kok M, Bron G, Erni B, Mukhija S.** 2003. Effect of enzyme I of the bacterial phosphoenolpyruvate: sugar phosphotransferase system (PTS) on virulence in a murine model. Microbiology **149:**2645–2652. http://dx.doi.org/10.1099/mic.0.26406-0.
54. **Molloy EM, Cotter PD, Hill C, Mitchell DA, Ross RP.** 2011. Streptolysin S-like virulence factors: the continuing *sagA*. Nat. Rev. Microbiol. **9:**670–681. http://dx.doi.org/10.1038/nrmicro2624.
55. **Gao J, Gusa AA, Scott JR, Churchward G.** 2005. Binding of the global response regulator protein CovR to the *sag* promoter of *Streptococcus pyogenes* reveals a new mode of CovR-DNA interaction. J. Biol. Chem. **280:**38948–38956. http://dx.doi.org/10.1074/jbc.M506121200.
56. **Hanahan D, Meselson M.** 1983. Plasmid screening at high colony density. Methods Enzymol. **100:**333–342.
57. **Miroux B, Walker JE.** 1996. Over-production of proteins in *Escherichia coli*: mutant hosts that allow synthesis of some membrane proteins and globular proteins at high levels. J. Mol. Biol. **290:**289–298. http://dx.doi.org/10.1006/jmbi.1996.0399.
58. **Aziz RK, Pabst MJ, Jeng A, Kansal R, Low DE, Nizet V, Kotb M.** 2004. Invasive M1T1 group A Streptococcus undergoes a phase-shift *in vivo* to prevent proteolytic degradation of multiple virulence factors by SpeB. Mol. Microbiol. **51:**123–134.
59. **Le Breton Y, Mistry P, Valdes KM, Quigley J, Kumar N, Tettelin H, McIver KS.** 2013. Genome-wide identification of genes required for fitness of group A Streptococcus in human blood. Infect. Immun. **81:**862–875. http://dx.doi.org/10.1128/IAI.00837-12.
60. **Ribardo DA, McIver KS.** 2006. Defining the Mga regulon: comparative transcriptome analysis reveals both direct and indirect regulation by Mga in the group A streptococcus. Mol. Microbiol. **62:**491–508. http://dx.doi.org/10.1111/j.1365-2958.2006.05381.x.